P H Y S I C A L R E V I E W L E T T E R S

Anderson Localization on the Bethe Lattice: Nonergodicity of Extended States

A. De Luca,[1] B. L. Altshuler,[2] V. E. Kravtsov,[3,4] and A. Scardicchio[2,3,5,6]

[1]*Laboratoire de Physique Théorique de l'ENS and Institut de Physique Theorique Philippe Meyer 24,
Rue Lhomond, 75005 Paris, France*
[2]*Physics Department, Columbia University, 538 West 120th Street, New York, New York 10027, USA*
[3]*Abdus Salam International Center for Theoretical Physics, Strada Costiera 11, 34151 Trieste, Italy*
[4]*L. D. Landau Institute for Theoretical Physics, 2 Kosygina Street, 119334 Moscow, Russia*
[5]*Physics Department, Princeton University, Princeton, New Jersey 08544, USA*
[6]*INFN, Sezione di Trieste, Strada Costiera 11, 34151 Trieste, Italy*

Statistical analysis of the eigenfunctions of the Anderson tight-binding model with on-site disorder on regular random graphs strongly suggests that the extended states are multifractal at any finite disorder. The spectrum of fractal dimensions $f(\alpha)$ defined in Eq. (3) remains positive for α noticeably far from 1 even when the disorder is several times weaker than the one which leads to the Anderson localization; i.e., the ergodicity can be reached only in the absence of disorder. The one-particle multifractality on the Bethe lattice signals on a possible inapplicability of the equipartition law to a generic many-body quantum system as long as it remains isolated.

Introduction.—Anderson localization (AL) [1,2], in its broad sense, is one of the central paradigms of quantum theory. Diffusion, which is a generic asymptotic behavior of classical random walks [3], is inhibited in quantum case and under certain conditions it ceases to exist [2]. This concerns quantum transport of noninteracting particles subject to quenched disorder as well as transport and relaxation in many-body systems. In the latter case the *many-body localization* (MBL) [4] can be thought of as localization in the Fock space of Slater determinants, which play the role of lattice sites in a disordered tight-binding model. In contrast to a *d*-dimensional lattice, the structure of Fock space is hierarchical [5]: a two-body interaction couples a one-particle excitation with three one-particle excitations, which in turn are coupled with five-particle excitations, etc. This structure resembles a random regular graph (RRG) - a finite size Bethe lattice (BL) without boundary. Interest to the problem of single particle AL on the BL [6,7] has recently revived [8–12] largely in connection with MBL. It is a good approximation to consider hierarchical lattices as trees where any pair of sites is connected by only one path and loops are absent. Accordingly the sites in resonance with each other are much sparser than in ordinary $d > 1$-dimensional lattices. As a result even the extended wave functions can occupy zero fraction of the BL, i.e., be nonergodic. The nonergodic extended states on three-dimensional lattices where loops are abundant are commonly believed [13–16] to exist but only at the critical point of the AL transition.

In this paper we analyze the eigenstates of the Anderson model on RRG with connectivity $K + 1$ (K is commonly used to refer to the branching of the corresponding BL) and N sites,

$$H = -\sum_{\langle ij \rangle}(c_i^\dagger c_j + \text{h.c.}) + \sum_i \varepsilon_i c_i^\dagger c_i, \qquad (1)$$

where $\varepsilon_i \in [-W/2, W/2]$. A normalized wave function $\psi(i)$ ($i = 1, ..., N$) can be characterized by the moments $I_q = \sum_i |\psi(i)|^{2q} \propto N^{-\tau(q)}$ [13] ($I_1 = 1$ for the normalization). One can define the ergodicity as the convergence in the limit $N \to \infty$ of the real space averaged $|\psi(i)|^{2q}$ (equal to I_q/N) to its ensemble average value $\langle |\psi(i)|^{2q} \rangle = \langle I_q \rangle / N$. This happens when the fluctuations of $|\psi(i)|^2$ are relatively weak and $\langle |\psi(i)|^{2q} \rangle = a(q)\langle |\psi(i)|^2 \rangle^q$ with $a(q) = O(N^0)$. Since $\psi(i)$ is normalized $\langle |\psi(i)|^2 \rangle = N^{-1}$ and thus $I_q = N\langle |\psi(i)|^{2q} \rangle = a(q)N^{1-q}$, i.e., $\tau(q) = q - 1$. The latter condition turns out to be both necessary and sufficient for the convergence of I_q to $\langle I_q \rangle$ (see the Supplemental Material [17] for the discussion). Deviations of $\tau(q)$ from $q - 1$ are signatures of the non-ergodic state. If the ratio $D_q = \tau(q)/(q - 1)$ depends on q, the wave function $\psi(i)$ is called *multifractal*. It is customary to characterize $\psi(i)$ by the spectrum of fractal dimensions (SFD) $f(\alpha)$ related to $\tau(q)$ by the Legendre transform: $\tau(q) = q\alpha - f(\alpha)$ with $\alpha(q)$ being a solution to $f'(\alpha) = q$ (see the Supplemental Material [17]). Such a relationship follows from the definition of $f(\alpha)$, Eq. (3), and the saddle-point approximation in evaluating of the moments I_q at large $\ln N$.

In this Letter we develop a method of extracting SFD $f(\alpha)$ from the numerical diagonalization of the Hamiltonian Eq. (1) on the RRG with finite number of

sizes N and branching $K = 2$. The multifractality is overshadowed by the fast oscillations $\phi_{osc}(i)$ of $\psi(i)$ which should be separated from the smooth envelope $\psi_{en}(i)$,

$$\psi(i) = \psi_{en}(i)\phi_{osc}(i). \qquad (2)$$

Below we describe how to separate the statistics of $\psi_{en}(i)$ and demonstrate that at all strengths W of the on-site disorder the distribution function (DF) of $x = N|\psi_{en}(i)|^2$ is consistent with the multifractal ansatz [14,16]; i.e., it can be expressed through SFD $f(\alpha)$ as

$$P(x) = \frac{A}{x}N^{f(\alpha)-1}, \qquad \alpha(x) = 1 - \ln x / \ln N, \qquad (3)$$

where $A \sim O(N^0)$ is the normalization constant. The SFD $f(\alpha)$ in Eq. (3) is known [13,16] to be a convex function equal to 1 at its maximum, $f_{max} = f(\alpha_0) = 1$. For ergodic states $f(\alpha) = -\infty$ unless $\alpha = 1$ where $f(1) = 1$, while a finite support $0 < \alpha_{min} < \alpha < \alpha_{max}$ where $f(\alpha) > 0$ is a signature of multifractality (nonergodicity).

We found that with decreasing disorder $f(\alpha)$ evolves from almost triangular shape in the insulator to a steep parabolic shape concentrated near $\alpha = 1$ (see Fig. 1).

Fractal behavior of quantum dynamics on the disordered BL have been discussed previously. Transmission from the root to a given surface point of the Cayley tree turns out to be multifractal [12]. This surface multifractality of the extended states does not necessarily mean that bulk of the BL is multifractal: it is known, e.g., that in two dimensions the bulk multifractality is much weaker than the surface one [16]. Our analysis of the results of exact numerical diagonalization of the Hamiltonian (1) on the RRG demonstrated that the extended wave functions are multifractal even in the bulk of the BL. Hopefully the tools developed in [8,9,18] might lead to a proof of the multifractality in the whole delocalized region, a possibility that we plan to explore in future work.
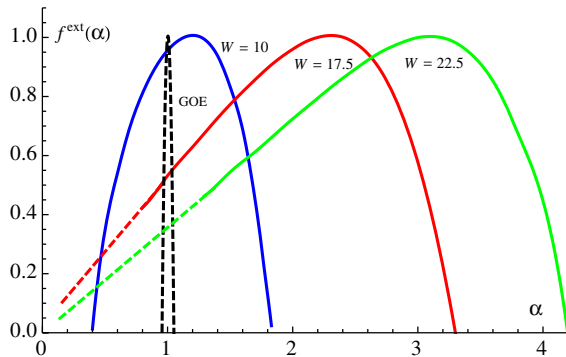

FIG. 1 (color online). Numerical results for $f(\alpha)$ on the RRG with the connectivity $K + 1 = 3$ after linear extrapolation $f(\alpha, N) = f^{ext}(\alpha) + c/\ln N$ to $1/\ln N \to 0$ for different values of disorder W. The dashed straight lines show the slope $k < 1/2$ for the localized ($W = 22.5$) and $k = 1/2$ for the critical ($W = 17.5$) states.

Authors of Ref. [11] analyzed numerically the statistics of the spectra and by population dynamics the distribution of the Green functions of the model (1) and conjectured a transition between extended-ergodic and extended non-ergodic phases in addition to the Anderson transition. Contrarily, we do not see any evidence of the second transition and believe that the entire extended phase is nonergodic.

Numerics on the BL: rectification and extrapolation.— With the exception of the deeply localized states discussed below, analytical methods to address the problem of wave function statistics on BL are yet to be developed. One can try to access these statistics numerically by diagonalization of the Anderson model Eq. (1) on a RRG. The first challenge along this route is the necessity to extract the statistics of the smooth envelope $\psi_{en}(i)$ of the wave function $\psi(i)$, Eq. (2). The short-range oscillations of $\phi_{osc}(i)$ have nothing to do with AL but dominate the numerically obtained DF of $|\psi(i)|^2$ at small $|\psi(i)|^2$. This tail of the DF thus reflects the density of the nodes of $\phi_{osc}(i)$ rather than the probability for $|\psi_{en}(i)|^2$ to be small.

Since the scales of spatial dependencies of $\psi_{en}(i)$ and $\phi_{osc}(i)$ are so different, it is natural to assume that these two functions are statistically independent and $|\phi_{osc}|^2$ is characterized by the Porter-Thomas DF of the Gaussian orthogonal ensemble (GOE) [19] $P_{GOE}(|\phi_{osc}|^2) = (\sqrt{2\pi}|\phi_{osc}|)^{-1}\exp(-|\phi_{osc}|^2/2)$. Under these assumptions $\tilde{\alpha} = 1 - \ln(N|\psi|^2)/\ln N$, which is evaluated numerically, is a sum of two statistically independent random variables: $\tilde{\alpha} = \alpha(x) + \alpha_{osc}$, where $\alpha(x)$ is given by Eq. (3) and $\alpha_{osc} = -\ln|\phi_{osc}|^2/\ln N$. The DF of $\tilde{\alpha}$ is thus a convolution of the DF $p(\alpha) = P(x(\alpha))x(\alpha)\ln N$ of $\alpha(x)$ with $\tilde{P}_{GOE}(\alpha_{osc}) = \ln N(2\pi N^{\alpha_{osc}})^{-1/2}\exp(N^{-\alpha_{osc}}/2)$; i.e., $P(x)$ determined by (3) can be obtained ("rectified") from the DF of $\tilde{\alpha}$ and by the Laplace transform method (see the Supplemental Material [17] for details).

Another, even bigger challenge is that Eq. (3) is expected to hold only in the limit of a sufficiently large graph; i.e. $f(\alpha)$ can be determined only from the limit of $f(\alpha, N) = f(\alpha) + \delta_N f(\alpha)$ at $\ln N \to \infty$, where

$$f(\alpha, N) = 2 - \alpha + \ln P(x)/\ln N, \qquad x = N^{1-\alpha}. \qquad (4)$$

The biggest number of sites accessible to us was $N = 32,000$. Increasing further N does not buy much, as the computation time increases as N^3 while the finite-size correction $\delta_N f(\alpha)$ is small only as $1/\ln N$. However, we found a bright side of the slowness of the convergence: in the broad interval of α the correction $\delta_N f(\alpha)$ turns out to be linear in $1/\ln N$ to a surprisingly high accuracy. This allowed us to make a reliable linear extrapolation in $1/\ln N$ well beyond the numerical data.

Fixed points in the N-dependence of $f(\alpha, N)$.—We numerically diagonalized the Hamiltonian Eq. (1) for the regular graph with connectivity $K + 1 = 3$ (which does not
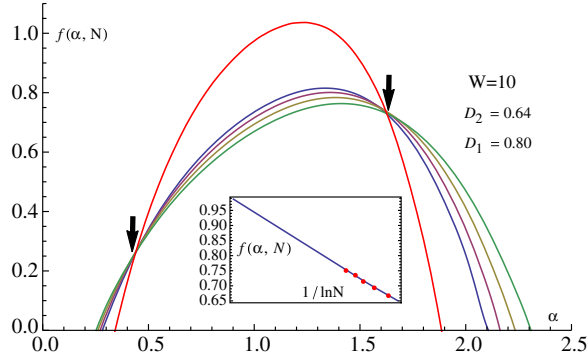
FIG. 2 (color online). N dependence of $f(\alpha, N)$ on the RRG with $K = 2$ for $N = 2, 4, 8, 16 \times 10^3$ (from green to blue in ascending order) in the extended phase $W = 10$. The $f^{\text{ext}}(\alpha)$ obtained by linear extrapolation of $f(\alpha, N)$ to $1/\ln N \to 0$ is shown by a thin red line. The maximal value $f_{\max} \approx 1.03$ of $f^{\text{ext}}(\alpha)$ is very close to the theoretical expectation $f_{\max} = 1$. We also show the fractal dimensions D_2 and $D_1 = \lim_{q \to 1+} D_q$ corresponding to $f^{\text{ext}}(\alpha)$. The plots for different N show apparent fixed points at $\alpha \approx 0.5$ and $\alpha \approx 1.6$ indicated by arrows. Similar fixed points with W-dependent positions are seen at any strength of disorder studied. This rules out that $f(\alpha, N)$ approaches at $\ln N \to \infty$ the ergodic limit $f(\alpha) = 1$ at $\alpha = 1$, $f(\alpha) = -\infty$ otherwise. In the insert: the linear extrapolation of $f(\alpha, N)$ for $\alpha = 1.0$; the red points show $f(\alpha = 1.0, N)$ at $N = 2, 4, 8, 16, 32 \times 10^3$.

contain boundary sites) extracting about 2% of the states around the center $E = 0$ of the spectrum, and evaluated $f(\alpha, N)$ for $N = 32, 16, 8, 4, 2 \times 10^3$ at several disorder strengths W, both above the Anderson transition at $W_c = 17.5$ and below it, down to $W = 5$. Plots of $f(\alpha)$ for $W = 10$ and $W = 5$ are shown in Fig. 2 and Fig. 3.

An important observation is the existence of two fixed points α_+ and α_- (shown by arrows): $f(\alpha_+, N)$ and $f(\alpha_-, N)$ are essentially N independent. This rules out the possibility of $f(\alpha)$ evolving with further increase of N into a sharp parabola at $\alpha = 1$ (dashed line in Fig. 1). In addition to that we verified to a high degree of accuracy that $\delta_N f(\alpha)$ is linear in $1/\ln N$, at least for $\alpha_- < \alpha < \alpha_+$. The insert of Fig. 2 demonstrates that the values of $f(\alpha = 1, N)$ being plotted as a function of $1/\ln N$ for $N = 32, 16, 8, 4, 2 \times 10^3$ (red points) form an almost ideal straight line which can be prolonged down to $1/\ln N = 0$. This is how we obtained the extrapolated SFD $f^{\text{ext}}(\alpha)$. It was already mentioned that the maximal value of $f(\alpha)$ in Eq. (3) should be 1. It is not the case for $f(\alpha, N)$ as one can see from Figs. 2,3. After extrapolation, however, the maxima of $f^{\text{ext}}(\alpha)$ turn out to be much closer to 1: $f^{\text{ext}}_{\max} = 0.99, 1.03, 1.01, 1.00$ for $W = 5, 10, 17.5, 22.5$, respectively. We just conclude that the extrapolation passed an important and nontrivial test for consistence.

Verification of the symmetry of $f(\alpha)$.—Another important observation providing us with the additional confidence in the validity of the extrapolation is the symmetry of SFD and DF,
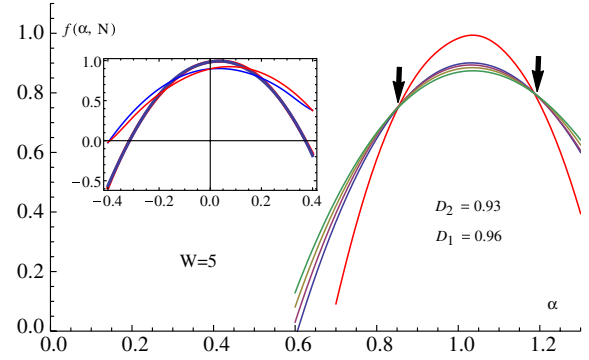

FIG. 3 (color online). $f^{\text{ext}}(\alpha)$ obtained by linear extrapolation (see Fig. 2) of $f(\alpha, N)$ to $1/\ln N \to 0$ (red) and $f(\alpha, N)$ for $N = 2, 4, 8, 16 \times 10^3$ at disorder strength $W = 5$. The fixed points are shown by arrows. In the insert: verification of the symmetry Eq. (5) for the extrapolated $f^{\text{ext}}(\alpha)$ (coinciding blue and red thick curves), and for $f(\alpha, N)$ at $N = 16 \times 10^3$ (distinctly different thin blue and red curves).

$$f(1 + \alpha) = f(1 - \alpha) + \alpha, \tag{5}$$

$$P(x) = x^{-3} P(x^{-1}). \tag{6}$$

One can use Eq. (3) to check that Eqs. (5) and (6) follow from each other. Log-normal distribution found for weakly multifractal states in two-dimensional disordered systems [20] is one of the examples of this symmetry. A relation similar to Eq. (6) was proven for the DF of the local density of states $\rho(i, \varepsilon)$ in a one-dimensional chain [21] and a variety of systems (e.g. short and long disordered wires, two-dimensional and three-dimensional disordered systems) described by the nonlinear sigma model [22,23]. The precise conditions of validity of Eq. (6) for the individual eigenfunctions are yet to be formulated. It does not hold for the localized eigenstates, while for weakly multifractal extended states in two-dimensional systems it is valid [20]. A vast numerical evidence of the validity of Eq. (5) for the multifractal states at the Anderson transition point in two-dimensional and three-dimensional systems was reported [16]. In the insert of Fig. 3 we present the separate plots of $f^{\text{ext}}(1 + \alpha)$ and $f^{\text{ext}}(1 - \alpha) + \alpha$ for the weakest disorder we studied, $W = 5$ (deep in the region of extended states, the fractal dimensions D_1 and D_2 are very close to 1). One can see that the two curves are indistinguishable in the interval $-0.4 < \alpha < 0.4$, while $f(1 + \alpha, N = 16 \times 10^3)$ and $f(1 - \alpha, N = 16 \times 10^3) + \alpha$ differ noticeably.

In the localized regime $W > W_c = 17.5$ and at the critical point $W = W_c$ the shape of the SFD is approximately triangular (see Fig. 1),

$$f^{\text{ext}}(\alpha) = k\alpha\theta(1 - k\alpha), \quad \theta(z) = \begin{cases} 1 & \text{if} \quad z > 0 \\ 0 & \text{if} \quad z < 0. \end{cases} \tag{7}$$

The slope k depends on the disorder $k = k(W)$ with $k(W_c)$ is very close to $1/2$. Note, that the only linear $f(\alpha)$ allowed

by Eq. (5) is the one with $k = 1/2$. Thus one concludes that the critical states with not very small amplitude of wave function (not very large α) for $W = W_c$ obey Eq. (5). At the same time, the most abundant critical states around the maximum value of $f(\alpha)$ reached at $\alpha = \alpha_0 \approx 2.3$ clearly violate the symmetry Eq. (5). Indeed $f(1 - \alpha)$ is defined only for $\alpha < 1$ and thus according to Eq. (5) $f(1 + \alpha)$ should make no sense for $\alpha > 1$. In the localized regime we found that α_0 increases with disorder, while $k(W) \approx \alpha_0^{-1}$ decreases below $1/2$. This is in a clear contradiction with Eq. (5).

Power-law DF for strongly localized states on BL.—Our numeric-based conclusions on the regime of strong localization $W \gg W_c$ fully agree with the analytical results which follow from the locator expansion [6] (also see the Supplemental Material [17]). In the shortest path approximation [24,25] one obtains $\psi^{(0)}(i) = \prod_{j \in p_{0,i}} (\varepsilon_0 - \varepsilon_i)^{-1}$, where $\psi^{(0)}(i)$ is the eigenfunction of the Hamiltonian Eq. (1) on BL which at $W = \infty$ is located on the site 0, and $p_{0,i}$ is the shortest path connecting sites 0 and i. One can show that within this approximation the DF $P(x)$ can be represented as

$$P(x) = I(1, 0) - N^{1-\kappa} I(1 - m, \kappa). \quad (8)$$

Here $m = \ln N / \ln K$ is the BL radius, $\kappa = \ln(W/2)/\ln K$, and

$$I(p, q) = \frac{1}{\sqrt{Nx^3}} \int_B \frac{ds}{4\pi i} \frac{s^p (xN^{2q-1})^{s/2}}{s - K^{\kappa(s-1)+1}}. \quad (9)$$

The contour $B \in (r - i\infty, r + i\infty)$ is parallel to the imaginary axis and crosses the real axis at $s_- < r < s_+$, where $s_\pm$ are the larger and the smaller of the only two real roots of the equation

$$s = K^{\kappa(s-1)+1}. \quad (10)$$

These roots can be shown to exist as long as $\kappa > \kappa_c = \ln(\kappa_c \ln K) + \ln(eK)/\ln K$, which can be rewritten as

$$W \geq W_c = 2eK \ln(W_c/2) \approx 2eK \ln(eK). \quad (11)$$

Solution of Eq. (11) is nothing but the critical disorder of Ref. [2] (see Eq. (84) there, see also the "upper limit critical condition" of Refs. [6,7]). Since $x = N|\psi(i)|^2 < N$ in the first term on the right-hand side of Eq. (8) one can deform the contour of integration in Eq. (9) to encircle the pole $s = s_+$. For the second term, $N^{1-\kappa} I(1 - m, \kappa)$, this can be done only provided that $x(N/K)^{2\kappa} < N$. Under this condition the two terms cancel each other and $P(x) \equiv 0$. In the opposite case $x > N(N/K)^{-2\kappa}$, the integral $I(1 - m, \kappa)$ in Eq. (9) is determined by the poles $s = s_-$ and $s = 0$. Within the region of validity of the shortest path approximation $\frac{s_-}{2} \ln x \sim \frac{2\kappa}{W} \ln N \ll 1$ the two contributions cancel each

other, i.e., $P(x) = I(1, 0)$. Finally within the shortest path approximation, for $W \gg W_c$ we have

$$P(x) = \frac{\theta(x - x_{\min})}{N^2} \left(\frac{x}{N}\right)^{(s_+ - 3)/2}, \quad (12)$$

where $x_{\min} = N^{1-2\kappa} K^{2\kappa} \Rightarrow \alpha_{\max} = 2\kappa(1 - m^{-1}) \approx 2\kappa$. Using the definition of $\alpha(x)$ Eq. (3) one obtains from the power-law DF Eq. (12) the linear SFD $f(\alpha)$, Eq. (7) with

$$k(W) = \frac{1}{2}(1 - s_+), \quad (13)$$

truncated at $\alpha > \alpha_{\max}$. Note that for $\kappa \gg 1$ (i.e., for $W \gg 2K$), Eq. (10) yields $s_+ \approx 1 - \kappa^{-1}$, so that the condition $k(W)\alpha_{\max} = 1$ encoded in Eq. (7) is satisfied at large disorder ($\kappa \gg 1$) and large system size ($m \gg 1$). Power-law distributions of wave function coefficients have been observed in many-body systems also in the delocalized region (see [26] where a criterion for ergodicity breaking based on them was proposed).

Conclusion.—We developed an effective method for extracting statistics of the smooth envelopes $\psi_{en}(i)$ of random eigenfunctions of the Anderson model (1) on RRG and to extrapolate these results from RRG to the BL with an infinite number of sites. Our results strongly suggests that DF of $|\psi_{en}(i)|^2$ in the limit $N \to \infty$ indeed converges to the form Eq. (3) regardless to the strength of disorder. As long as the states are localized the spectrum of fractal dimensions turns out to be triangular: $f(0) = 0$ and the linear $f(\alpha)$ is well described by Eq. (7). The slope k increases as the disorder W decreases and reaches its maximal possible value $k_c = 1/2$ at the Anderson transition point $W = W_c = 17.5$. With further decrease of the disorder below the critical one $f(\alpha)$ gradually crosses over to the parabolic shape typical for weak multifractality: the two roots of $f(\alpha)$ become positive $0 < \alpha_{\min} < 1 < \alpha_{\max}$ ($\alpha_{\min} \to 0^+$ as $W \to W_c^-$). However even for W several times smaller than W_c both $\alpha_{\min}$ and $\alpha_{\max}$ turn out to be quite far from 1, while the ergodicity would imply that $\alpha_{\min}, \alpha_{\max} \to 1$. We conclude that the nonergodicity and multifractality persist in the entire region of delocalized states $0 < W < W_c$, and the only critical point is the point of the Anderson localization transition.

It goes without saying that only RRG with not too big N are accessible for the numerical analysis and one has to deal with $f(\alpha, N)$ determined by Eq. (4). However the existing data allow us to exclude the possibility that the observed nonergodicity is a finite size effect. Our confidence is based, among other things, on the existence of two fixed points: $f(\alpha, N)$ is N independent at $\alpha = \alpha_-(W) < 1$ and $\alpha = \alpha_+(W) > 1$. The extrapolation of $f(\alpha, N)$ to $N \to \infty$ in the interval $\alpha_- \leq \alpha \leq \alpha_+$ turned out to be tremendously reliable. It is thus hard to imagine how $f(\alpha, N)$ could evolve to the ergodic limit with further increase of N.

Another argument in favor of the true nonergodicity is that the behavior of $f(\alpha, N)$ Eq. (4) is not a critical behavior: $f(\alpha, N)$ depends on both N and W in a broad range of these variables. Indeed the critical behavior, which was analytically predicted in [27,28] for sparse random matrices (SRM) implies that at $W < W_c$ the eigenvectors are ergodic or multifractal correspondingly for $N > N_c(W)$ and for $N < N_c(W)$ (the critical volume $N_c(W)$ diverges as $W \to W_c$). Therefore $f(\alpha, N)$ depends either on N (in the critical regime) or on W, but never on both N and W. The reasons why the results of Refs. [27,28] do not apply to the RRG eigenvectors will be discussed elsewhere.

The absence of ergodicity for the dynamics of the one-particle Anderson model on the BL, in light of the possible connection with the many-body dynamics, suggests serious implications on the statistical mechanics of isolated systems with a large number of degrees of freedom. If the same phenomenon occurs in the many-body case, the equipartition law is likely not to be valid exactly even for strongly nonintegrable systems.

[1] E. Abrahams, *50 years of Anderson Localization* (World Scientific, Singapore, 2010), Vol. 24.
[2] P. W. Anderson, Phys. Rev. **109**, 1492 (1958).
[3] A. Einstein, Ann. Phys. (Berlin) **322**, 549 (1905).
[4] D. Basko, I. Aleiner, and B. Altshuler, Ann. Phys. (New York) **321**, 1126 (2006).
[5] B. L. Altshuler, Y. Gefen, A. Kamenev, and L. S. Levitov, Phys. Rev. Lett. **78**, 2803 (1997).
[6] R. Abou-Chacra, D. Thouless, and P. Anderson, J. Phys. C **6**, 1734 (1973).
[7] R. Abou-Chacra and D. Thouless, J. Phys. C **7**, 65 (1974).
[8] M. Aizenman, R. Sims, and S. Warzel, Commun. Math. Phys. **264**, 371 (2006).
[9] M. Aizenman and S. Warzel, Europhys. Lett. **96**, 37004 (2011).
[10] G. Biroli, G. Semerjian, and M. Tarzia, Prog. Theor. Phys. Suppl. **184**, 187 (2010).
[11] G. Biroli, A. Ribeiro-Teixeira, and M. Tarzia, arXiv:1211.7334.
[12] C. Monthus and T. Garel, J. Phys. A **44**, 145001 (2011).
[13] F. Wegner, Z. Phys. B **44**, 9 (1981).
[14] B. L. Altshuler, V. E. Kravtsov, and I. V. Lerner, JETP Lett. **43**, 441 (1986).
[15] V. E. Kravtsov, I. V. Lerner, B. L. Altshuler, and A. G. Aronov, Phys. Rev. Lett. **72**, 888 (1994).
[16] F. Evers and A. D. Mirlin, Rev. Mod. Phys. **80**, 1355 (2008).
[17] See the Supplemental Material at http://link.aps.org/supplemental/10.1103/PhysRevLett.113.046806 for more details on the multifractal analysis leading to the numerical determination of $f(\alpha, N)$ in Eq. (4) and an analytic proof (within the forward approximation) of Eqs. (7)–(12)
[18] M. Aizenman and S. Warzel, J. Eur. Math. Soc. **15**, 1167 (2013).
[19] M. L. Mehta, *Random Matrices*, (Academic, New York, 2004), Vol. 142.
[20] V. I. Fal'ko and K. B. Efetov, Phys. Rev. B **52**, 17413 (1995).
[21] B. L. Altshuler and V. N. Prigodin, Zh. Eksp. Teor. Fiz. **95**, 348 (1989).
[22] A. D. Mirlin and Y. V. Fyodorov, Phys. Rev. Lett. **72**, 526 (1994).
[23] A. D. Mirlin and Y. V. Fyodorov, J. Phys. I (France) **4**, 655 (1994).
[24] E. Medina and M. Kardar, Phys. Rev. B **46**, 9984 (1992).
[25] J. D. Miller and B. Derrida, J. Stat. Phys. **75**, 357 (1994).
[26] A. De Luca and A. Scardicchio, Europhys. Lett. **101**, 37003 (2013).
[27] Y. V. Fyodorov and A. D. Mirlin, Phys. Rev. Lett. **67**, 2049 (1991).
[28] A. D. Mirlin and Y. V. Fyodorov, Phys. Rev. B **56**, 13393 (1997).